Light-induced properties of ruthenium-doped Bi 4 Ge 3 O 12 crystals

Vera Marinova, Shiuan Huei Lin, and Ken Yuh Hsu

Articles you may be interested in

Photoinduced absorption study of carrier dynamics in Ru-doped Bi 12 SiO 20 crystals after nanosecond laser pulse excitation
J. Appl. Phys. **107**, 113106 (2010); 10.1063/1.3418443

Phenomenological characterization of photoactive centers in Bi 12 Ti O 20 crystals
J. Appl. Phys. **101**, 043101 (2007); 10.1063/1.2434009

Third-order nonlinearities of Bi 12 GeO 20 crystal measured by nanosecond radiation
J. Appl. Phys. **97**, 104303 (2005); 10.1063/1.1891280

Twelve-fold increase of diffraction efficiency of thermally fixed holograms in Bi 12 SiO 20
J. Appl. Phys. **97**, 073505 (2005); 10.1063/1.1875744

Direct measurement of the dispersion of the electrogyration coefficient of photorefractive Bi 12 Ge O 20 crystals
J. Appl. Phys. **97**, 023531 (2005); 10.1063/1.1828585

Light-induced properties of ruthenium-doped Bi$_4$Ge$_3$O$_{12}$ crystals

Vera Marinova[a)]
Department of Photonics & Institute of Electro-optical Engineering, National Chiao Tung University, 1001 Ta Hsueh Road, Hsinchu 30050, Taiwan

Shiuan Huei Lin
Department of Electrophysics, National Chiao Tung University, 1001 Ta Hsueh Road, Hsinchu 30050, Taiwan

Ken Yuh Hsu
Department of Photonics & Institute of Electro-optical Engineering, National Chiao Tung University, 1001 Ta Hsueh Road, Hsinchu 30050, Taiwan

The influence of ruthenium addition at different doping concentrations on the optical properties and holographic behavior of Bi$_4$Ge$_3$O$_{12}$ crystals is investigated. Doped Bi$_4$Ge$_3$O$_{12}$ single crystals are grown by using the Czochralski technique. The distribution coefficient of each crystal is measured to determine the concentration of a doped ruthenium element. Holographic experiments are performed. Ruthenium is found to make Bi$_4$Ge$_3$O$_{12}$ sensitive in the red spectral range. Thermal annealing and ultraviolet exposure have been used to modify the defect structure and corresponding absorption band of each crystal such that the holographic recording has been influenced. The diffraction efficiency increases with increasing of ruthenium content, especially after irradiation by ultraviolet light. © *2005 American Institute of Physics*. [DOI: 10.1063/1.2140869]

I. INTRODUCTION

Photorefractive crystals have many potential applications, such as high-density data storage, optical information processing, image amplification, phase conjugation, etc.[1,2] One of the fundamental issues for the success of these applications is to improve the photorefractive performance.

Since the photorefractive phenomenon results from the generation of suitable defects in the crystal structure, the creation of defects is an effective way to enhance the photorefractive effect. These defects can be generated by an appropriate doping element, by nonstoichiometric crystal growth, or by thermal annealing at different atmospheres. Meanwhile, the impurities can act as donors or acceptors for charge carriers, depending on impurities concentration, valence state, distribution coefficient, occupied site symmetry, etc. For different crystals, there is a different efficient method to create defects and change the characters of impurities.

Bismuth germanate, Bi$_4$Ge$_3$O$_{12}$, commonly abbreviated as BGO (2:3), belongs to the 43 m cubic point symmetry group and is known also as eulytine. It is colorless, transparent, and insoluble in water. Large crystals with a very good optical quality are readily available.[3,4] BGO crystals find practical applications as scintillator materials because of their room temperature (RT) luminescence,[5] as well as in optoelectronics as voltage and electric field sensors.[6] Furthermore, undoped BGO crystal is one of the few crystals in which it is possible to record holographic gratings at shorter ultraviolet (UV) wavelengths at room temperature.[7]

In order for the photorefractive sensitivity to be im-

proved and to produce the refractive index change in a visible spectral range, appropriate dopants could be added to the BGO structure. The BGO crystal has a large energy gap, which appears to be a suitable matrix for extrinsic impurities, such as transition metals and/or rare-earth elements. The existence of a photorefractive effect in the blue–green spectral interval by adding appropriate doping elements is demonstrated by many experimental works. The holographic gratings were recorded in Cr-doped BGO crystals at 442 nm,[8] in Fe-doped and Mn-doped BGO crystals in a blue–green spectral interval,[9] as well as in Co-doped BGO crystals at 488 nm.[10] Recently, holographic gratings were recorded in ruthenium-doped BGO crystal plates using 514 nm light.[11] In addition, a photochromic effect was also observed. Recently, the combination of photorefractive and photochromic effects has been extensively used in holographic data storage, and for such an application it is important for the induced absorption changes to be fully reversible.[12]

In the present article we study the influence of Ru on the optical and holographic properties of BGO crystals at a light wavelength of 633 nm after preliminary thermal annealing or UV illumination treatments. The results show that Ru-doped BGO crystals possess a photorefractive effect in this particular wavelength and demonstrate the possibility of extending the photorefractive sensitivity of a doped BGO crystal into the red spectral range.

II. EXPERIMENTAL DETAILS

Ru-doped BGO crystals were grown by using the Czochralski technique, with the aid of an automatic diameter–weight control. Stochiometric Bi$_2$O$_3$:GeO$_2$ powders were mixed in molar proportion 2:3. Ruthenium was introduced to the melt solution during the crystal growth in

---

TABLE I. Summary of Ru-doped $Bi_4Ge_3O_{12}$ crystal parameters.

Notation	Ru concentration $\times 10^{18}$ cm^{-3}	Dimensions $a \times b \times c^a$ (mm)^3
BGO:Ru(I)	1.1	$9.5 \times 9.5 \times 6$
BGO:Ru(II)	6.1	$9.5 \times 9.5 \times 9$

^{a}Thickness.

the form of RuO_2 oxide. The ruthenium concentrations in the grown crystals, determined by inductively coupled plasma atomic absorption spectrometry, are given in Table I. According to Table I, samples with a low and high ruthenium content are denoted as BGO:Ru(I) and BGO:Ru(II), respectively.

The distribution coefficient κ represents the ratio between the molar concentration of the Ru in the crystal (the nominal doping level) and the molar concentration of the same element in the melt solution (the actual doping level). The distribution coefficient of Ru in our BGO crystals was obtained to be 0.11.

Optical transmission spectra were measured in the wavelength range 280–800 nm using a Cary 5E model spectrophotometer. Reflection spectra were measured on plates with one polished and one ground side, in a visible spectrum using a Perkin-Elmer 330 spectrophotometer with special references for calibration at 488, 514.5, 576, 633, and 672 nm.

The absorption coefficient α (cm^{-1}) of the crystal plate after UV exposure and after thermal annealing was calculated by using the following formula:

$$T = \frac{(1-R^2)\exp(-\alpha d)}{1 + R^2 \exp(-2\alpha d)}, \tag{1}$$

where T is the transmission coefficient, R the reflection coefficient, and d is the crystal thickness.

The UV source was an arc lamp and the whole spectrum of the lamp was used in order to have the maximum UV output of $I=0.63$ W/cm^2. In the bleaching process, thermal annealing for 1 h at 450 °C in the oxygen atmosphere (thermal bleaching) was used.

Holographic gratings were carried out with a standard two-wave mixing setup. BGO:Ru(I) and BGO:Ru(II) parallelepipeds with edges, oriented with respect to the crystallographic [110], [$\bar{1}$10] and [001] directions were prepared for holographic experiments. The crystals dimensions are listed in Table I. The holographic recording geometry was set up as a transmission grating using a 633 nm He-Ne laser light. The angle θ between the two writing beams was 15° and the grating vector was perpendicular to the [001] direction. During the writing, one of the recording beams (signal beam) was blocked for about 0.1 s in every 5 s and the other beam (the reference beam) was used to monitor the grating buildup. During the erasure, only the reference beam was incident on the crystal by completely blocking the signal beam with a shutter. The diffraction efficiency η was defined as the ratio between the diffracted intensity and the input beam intensity by taking into account the surface reflection.
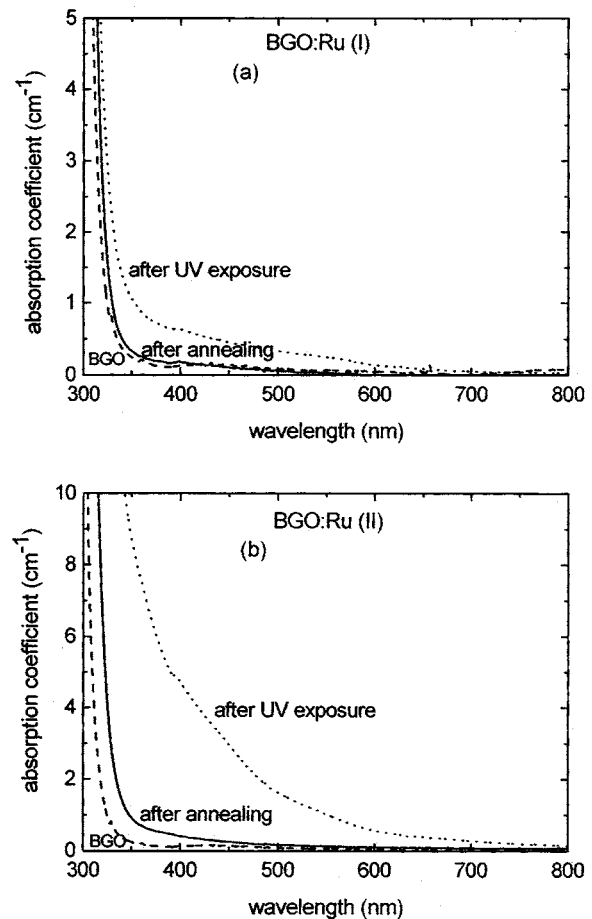

FIG. 1. Absorption coefficient α (cm^{-1}) dependence on the wavelength λ (nm) of BGO crystals, doped with different concentrations of ruthenium: (a) BGO:Ru(I) and (b) BGO:Ru(II). A straight line is after annealing at 450 °C; a dotted line is after UV exposure for 30 min. The absorption spectrum of undoped BGO is presented for reference (dashed line).

No external electric field was applied. The samples were thermally annealed after each experiment in order to empty all possible defect traps.

III. RESULTS AND DISCUSSION

Ruthenium-doped BGO crystal samples were slightly yellowish colored. The optical absorption spectra of Ru-doped BGO, measured after UV exposure and after thermal annealing, are shown in Figs. 1(a) and 1(b) for a low and high Ru concentration, respectively. The absorption coefficient of undoped BGO is also presented in Fig. 1 for comparison. As it is shown, a low concentration of Ru does not change the absorption shoulder of BGO; however, with higher Ru concentration, the optical absorption is shifted to the visible spectral range. Even in the bleached state the optical absorption in highly Ru-doped BGO crystal is larger than that of undoped BGO crystal. The changes in the absorption increase with the Ru content—the higher the ruthenium doping level, the larger the absorption coefficient. To measure the absorption spectra after UV exposure, the samples are illuminated with UV light for about 30 min. The results, as illustrated in Fig. 1, show that the UV irradiation induces visible absorption change that extends from $\lambda = 700$ nm up to the absorption edge. The photochromic mag-
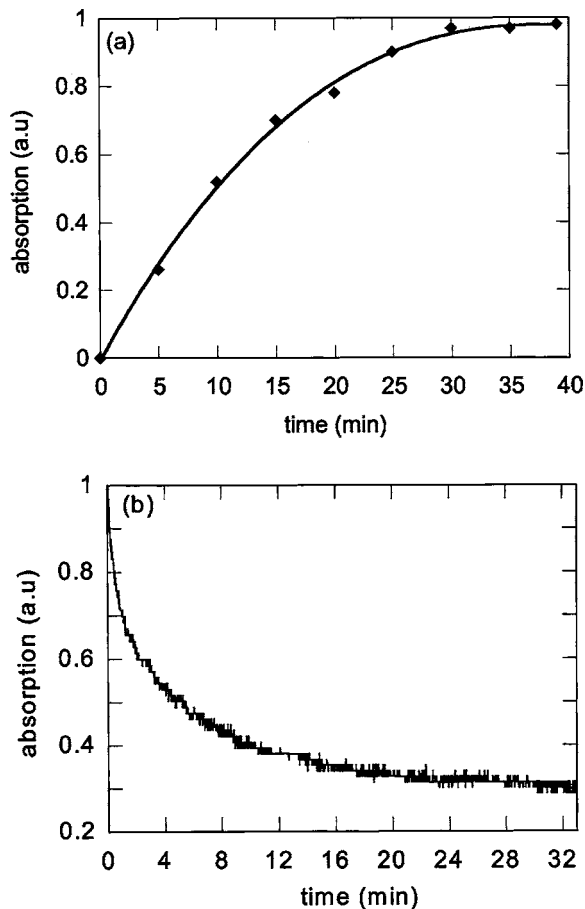
FIG. 2. The optical coloration dynamics in a BGO:Ru(II) sample using UV light with $I=0.63$ W/cm^2 (a) and an optical bleaching process using 2.7 eV light (b).
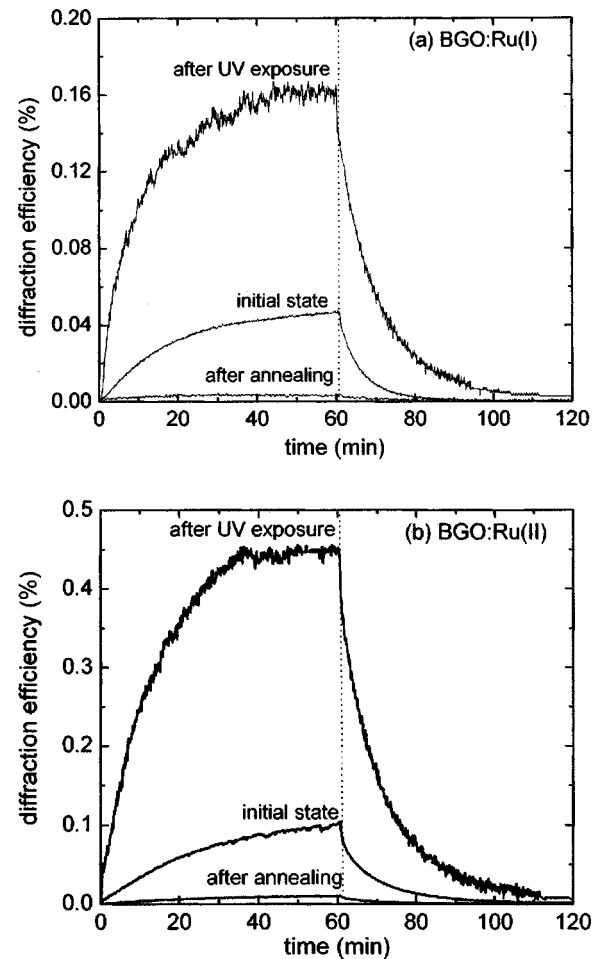

FIG. 3. The diffraction efficiency evolution during holographic recording and erasure at wavelength $\lambda=633$ nm for (a) BGO:Ru(I) and (b) BGO:Ru(II) crystals after annealing, at an initial state and after UV illumination. Grating spacing $\Lambda=0.61$ μm, recording intensity $I=38$ mW/cm^2, no external electric field.

nitude, which is defined as the difference of the crystal absorption after UV exposure and after thermal annealing, increases with the Ru concentration. We anticipate that this absorption change is probably due to the valence change of Ru caused by the photoinduced charge transfer from the UV sensitive absorption centers to the visible-light sensitive absorption centers via the conduction (valence) band. We suppose that the ruthenium ions increase the effective trap center concentration in a BGO structure and, as a consequence, the absorption throughout the investigated spectral range increases with the donor concentration.

Furthermore, the UV-induced defects are stable at room temperature. The colored crystals recovered their transparency by thermal annealing or by illumination with visible light. The response to UV light is fast and the induced absorption almost reached saturation in several minutes for highly Ru-doped BGO, as shown in Fig. 2(a). However, when using the same light intensity, the optical bleaching process was much slower than the coloration one. Figure 2(b) shows the optical bleaching dynamics by using 457 nm (2.7 eV) for the same sample. The absorption of the crystal changed very quickly in the beginning (0–16 min) and then very slowly decayed. Several hours were necessary for the crystal to become transparent. In these two experiments, a weak beam with the wavelength of 633 nm from a monochromator was used as the probe beam.

The photochromism in BGO crystal is associated mainly with the presence of dopant since the undoped BGO crystal does not exhibit any appreciable photochromic effect. The absorption coefficient change obtained in highly Ru-doped BGO is lower than the absorption coefficient change achieved in the case of Mn- and Fe-doped BGO, and very similar to those reported for BGO:Co.[13] Unfortunately, the valence state of Ru in BGO crystals in not known yet, however, Ru could exist in different valence states depending on its position in the crystal lattice, temperature, irradiation, etc. If the Ru exists in three different valence states Ru$^{3+/4+/5+}$ (as it does in similar cubic oxide crystals),[14] it is possible to assume that Ru^{4+} can trap the carriers, changing its valence to Ru^{3+} and Ru^{5+}, depending on whether electrons or holes are considered.

The holographic recording dynamics strongly depends on the history of the crystals. Figures 3(a) and 3(b) compare the recording and erasure characteristics measured after annealing, after UV exposure, and when the samples are in their initial state (without any preliminary treatments such as UV irradiation or thermal annealing). As shown in Fig. 3, when the crystals are in a bleached state, the diffraction efficiency is much lower than in the other two cases. Mean-
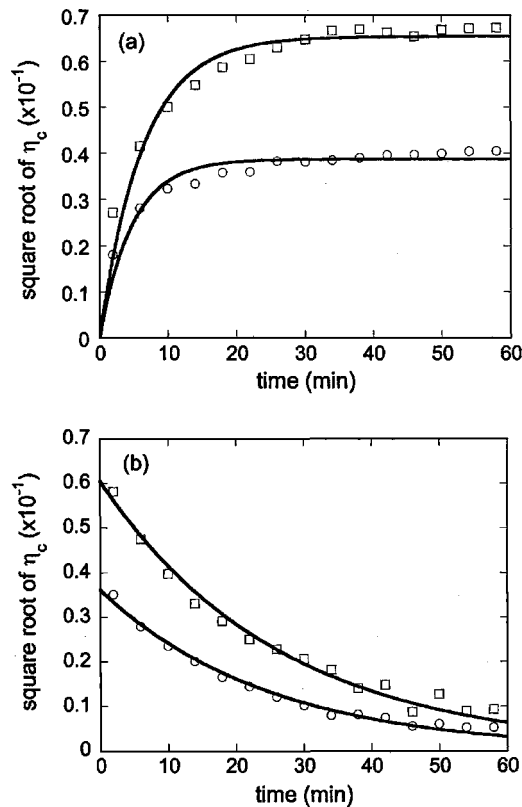
FIG. 4. Temporal behavior of the square root of diffraction efficiency during the writing process (a) and the erasure process (b) for BGO:Ru(I)—circles and BGO:Ru(II)—rectangular symbol. The symbols □ and ○ illustrate the measured data; the solid curves represent best fit to the experimental data.

while, after UV irradiation, the diffraction efficiency increases by more than four times in the case of highly Ru-doped BGO, compared to the sample without preliminary treatment.

The refractive index modulation Δn was calculated from the experimental diffraction efficiencies (shown in Fig. 3) by taking into account the surface reflection and by using Kogelnik's formula:[15]

$$\eta = \exp\left(-\frac{\alpha d}{\cos\theta}\right)\sin^2\left(\frac{\pi \Delta n\, d}{\lambda \cos\theta}\right), \qquad (2)$$

where α is the absorption coefficient, d is the crystal thickness, λ is the vacuum light wavelength, and θ is the angle between the two recording beams inside the crystal. For the crystals processed by the UV exposure, the maximum induced refractive index modulation of the BGO:Ru(1) crystal was $\Delta n = 1.7 \times 10^{-6}$ and that of the BGO:Ru(II) crystal was $\Delta n = 3.2 \times 10^{-6}$, respectively. The crystal with a higher Ru concentration shows both higher diffraction efficiency and larger refracted index changes. The refractive index change increase could be attributed to the presence of more trap centers in the highly Ru-doped BGO crystal, which provide a larger donor concentration for photorefractivity.[16] These changes are similar to those reported by Moya et al. for Cr-doped BGO, where the achieved refractive index modulation was $\Delta n = 1.89 \times 10^{-5}$ using laser irradiation with wavelength of 442 nm.[8]

Figures 4(a) and 4(b) show the temporal evolution of the

square root of the calculated diffraction efficiency η_c for two Ru concentrations after UV illumination during the grating buildup (a) and erasure (b) processes. The diffraction efficiency is calculated from the experimental diffraction efficiency by taking into account the surface reflection and the absorption of the crystal. The straight lines are the best fits to the experimental results, using the equations, which describe the square root of calculated diffraction efficiency behavior in writing and erasure regimes:

$$\sqrt{\eta_c} = \sqrt{\eta_{c\ \text{sat}}}[1 - \exp(-t/\tau_r)], \qquad (3)$$

$$\sqrt{\eta_c} = \sqrt{\eta_{c\ \text{sat}}}\exp(-t/\tau_e), \qquad (4)$$

where τ_r and τ_e are writing and erasure time constants, respectively. The $\eta_{c\ \text{sat}}$ is the saturation of the calculated diffraction efficiency. Figure 4 shows that the simple exponential law can fit the experimental data very well. These writing and erasure behaviors are typical for a photorefractive effect with a single impurity level.[16]

The observed diffraction efficiency temporal behavior resembles that reported for undoped and Cr-doped BGO crystals, and is slightly different from those of Fe- and Mn-doped crystals, where the writing dynamics is more complicated, starting with fast growth decreasing and finally approaching the steady-state value. The later behavior was explained, assuming that the compensating space-charge field created a secondary space-charge grating, which was not observed in a Ru-doped BGO crystal. From the theoretical fit we calculated the writing time constant to be $\tau_r = 4.8$ min and erasure time constant to be $\tau_e = 24$ min for BGO:Ru(I); and $\tau_r = 6.4$ min and $\tau_e = 26$ min for BGO:Ru(II), respectively. Here, the writing time constants of both crystals are similar. We believe that the donor and acceptor concentrations increased simultaneously so that both crystals have the similar concentrations of the photoexcited carrier density in the conduction band, which is the main factor to determine the writing time constant in the photorefractive crystal.[16]

These results show that Ru doping induces a shallow trap density in BGO crystals so that the holographic recording wavelength of the crystal can be extended to the red spectral range. The highly Ru-doped BGO crystal has a larger light-induced absorption change during UV illumination and refractive index change during holographic recording, which both phenomena indicate that more trap centers exist in such a crystal.[17] In the BGO crystal structure, each Ge^{4+} ion is coordinated by four oxygen ions, forming a tetrahedron, and each Bi^{3+} ion is coordinated by six oxygen ions. We suppose that Ru can replace Ge^{4+} ions in the tetrahedral position, as well as occupy other lattice sites. Furthermore, depending on the Ru concentration, it is possible for the oxygen content to be changed. The origin of photochromic and photorefractive centers still requires more experimental verifications. However, due to the ability of Ru-doped BGO to record photorefractive gratings at the red

spectral range, we hope that, with an increasing Ru concentration, it would be possible for the photorefractive characteristics to be optimized.

IV. CONCLUSIONS

BGO single crystals doped with two concentrations of Ru were grown successfully by using the Czochralski technique. It was found that the Ru addition to the BGO crystal structure generates sufficient density of suitable traps for photoinduced charge carriers in the red spectral range. The absorption and the effective trap densities increase with Ru concentration. Photorefractive behavior has been observed in Ru-doped BGO crystals at 633 nm. The states of the trap centers in Ru-doped BGO crystals can be manipulated by UV or visible light illumination. Thus, these crystals have the potential for nonvolatile holographic storage, using a two-step sensitization method.

ACKNOWLEDGMENTS

[1] H. J. Coufal, D. Psaltis, and G. T. Sincerbox, in *Holographic Data Storage* (Springer, Berlin, 2000).

[2] P. Gunter and J. P. Huignard, in *Photorefractive Materials and Their Applications I* (Springer, Berlin, 1988).

[3] B. C. Grabmaier, IEEE Trans. Nucl. Sci. **NS-31**, 372 (1984).

[4] P. A. Williams, A. H. Rose, K. S. Lee, D. C. Conrad, G. W. Day, and P. D. Hale, Appl. Opt. **35**, 3562 (1996).

[5] S. G. Raymond and P. D. Townsend, J. Phys.: Condens. Matter **12**, 2103 (2000).

[6] O. Kamada and K. Kakishita, Jpn. J. Appl. Phys., Part 1 **32**, 4288 (1993).

[7] G. Montemezzani, St. Pfandler, and P. Gunter, J. Opt. Soc. Am. B **9**, 1110 (1992).

[8] E. Moya, L. Contreras, and C. Zaldo, J. Opt. Soc. Am. B **5**, 1737 (1988).

[9] C. Zaldo, E. Moya, F. Magana, L. Kovacs, and K. Polgar, J. Appl. Phys. **73**, 2114 (1993).

[10] C. Zaldo and E. Dieguez, Opt. Mater. (Amsterdam, Neth.) **1**, 171 (1992).

[11] V. Marinova, S. H. Lin, M. L. Hsieh, K. Y. Hsu, M. Gospodinov, and V. Sainov, J. Mater. Sci.: Mater. Electron. **14**, 857 (2003).

[12] K. Buse, A. Adibi, and D. Psaltis, Nature (London) **393**, 665 (1998).

[13] H. Bou Rjeily, F. Ramaz, D. Petrova, M. Gospodinov, and B. Briat, Proc. SPIE **3178**, 169 (1997).

[14] L. Kovacs, E. Moya, K. Polgar, F. J. Lopez, and C. Zaldo, Appl. Phys. A **52**, 307 (1991).

[15] H. Kogelnik, Bell Syst. Tech. J. **48**, 2909 (1969).

[16] P. Yeh, *Introduction to Photorefractive Nonlinear Optics* (Wiley Interscience, New York, 1993), Chap. 3.

[17] P. Nouchi, J. P. Partanen, and R. W. Hellwarth, Phys. Rev. B **47**, 15581 (1993).